



Cold dense magnetopause boundary layer under northward IMF: Results from THEMIS and MHD simulations

Wenhui Li,¹ Joachim Raeder,¹ Marit Øieroset,² and Tai D. Phan²

Received 14 June 2008; revised 1 November 2008; accepted 8 December 2008; published 3 February 2009.

[1] A layer of nearly stagnant cold dense plasma is observed by THEMIS spacecraft in a closed field region immediately inside the dayside magnetopause near the low-latitude boundary layer on 3 June 2007. Using the OpenGGCM global MHD magnetosphere numerical model, we successfully reproduce this observed cold dense plasma layer in the simulation. The simulation results show that reconnection first occurs poleward of the cusp in the northern hemisphere, creating new open field lines extending southward and forming an open field layer; then subsequently occurs in the other hemisphere, creating new closed field lines that capture the magnetosheath plasma and form the dayside cold dense plasma layer. In this event, the open layer and the skin of the cold dense plasma layer have a southward tangential flow while the inner part of the cold dense plasma layer has a more stagnant and more turbulent flow.

Citation: Li, W., J. Raeder, M. Øieroset, and T. D. Phan (2009), Cold dense magnetopause boundary layer under northward IMF: Results from THEMIS and MHD simulations, *J. Geophys. Res.*, *114*, A00C15, doi:10.1029/2008JA013497.

1. Introduction

[2] It has been observed that some regions of the plasma sheet are dense ($>\sim 1 \text{ cm}^{-3}$) and cold ($<\sim 1 \text{ keV}$) for extended northward IMF periods [Fairfield *et al.*, 1981; Lennartsson and Shelley, 1986; Baumjohann *et al.*, 1989; Lennartsson, 1992]. The WIND and Geotail spacecraft recently provided more observations of the cold dense plasma sheet (CDPS) [Terasawa *et al.*, 1997; Fujimoto *et al.*, 1998; Phan *et al.*, 1998, 2000; Nagata *et al.*, 2007; Nishino *et al.*, 2007a, 2007b]. Wing and Newell [2002] examined the spatial extent of the cold dense ions under northward IMF using data from low-altitude DMSP satellites. Øieroset *et al.* [2005, 2008b] reported an unusually long lasting event observed by Cluster. The CDPS may have a significant impact on geomagnetic effects by providing a precondition for a following geomagnetic storm [Borovsky *et al.*, 1997; Denton *et al.*, 2006; Lavraud *et al.*, 2006a; Liemohn *et al.*, 2008].

[3] Most of the CDPS observations are made near the Earth in the tail ($X_{GSE} > -30 R_E$). The CDPS is often observed when the IMF has been northward, on average, for several hours. This plasma is characterized by high density ($\sim 1 \text{ cm}^{-3}$), low temperature ($<1 \text{ keV}$), and small flow velocity; it is found to be on closed field lines [Fujimoto *et al.*, 1998]. Terasawa *et al.* [1997] determined that the CDPS could be a temporal state of the plasma sheet. Many observations show that the cold dense plasma is located much more often near the flanks [e.g., Fujimoto *et al.*, 1996,

1998; Phan *et al.*, 1998; Fuselier *et al.*, 1999; Øieroset *et al.*, 2002] than at the center of the plasma sheet. This cold and dense plasma sheet has been detected deep inside the magnetosphere [Borovsky *et al.*, 1997; Thomsen *et al.*, 2003; Lavraud *et al.*, 2005a, 2006c] and often consists of a mixture of magnetosheath and magnetospheric plasma [e.g., Fujimoto *et al.*, 1996; Fuselier *et al.*, 1999; Nishino *et al.*, 2007a]. During prolonged periods of strongly northward IMF, the CDPS can fill the entire near-Earth plasma sheet [Øieroset *et al.*, 2005; Wing *et al.*, 2006].

[4] The ionosphere is unlikely to be the main source of this plasma since (1) the ionospheric outflow has been found to be strongest during active times and for southward IMF [Yau *et al.*, 1985; Øieroset *et al.*, 1999], and (2) the CDPS has been found to be absent a cold O^+ component [e.g., Rème *et al.*, 2001]. Therefore, the plasma entering the plasma sheet when the IMF is northward is believed to originate primarily from the solar wind.

[5] A number of processes have been proposed to account for the transfer of solar wind plasma into the magnetosphere [e.g., Sibeck *et al.*, 1999; Hultqvist *et al.*, 1999; Walker *et al.*, 1999], including direct cusp entry, finite gyroradii effect, wave-particle interaction, turbulence, impulsive penetration, and gradient drift [e.g., Axford and Hines, 1961; LeMaire, 1977; Treumann, 1997; Thorne and Tsurutani, 1991; Tsurutani *et al.*, 2003; Zhou *et al.*, 2007]. The following two mechanisms are considered to be the main processes that can transport the magnetosheath plasma into the magnetosphere under northward IMF conditions:

[6] 1. High-latitude reconnection in both hemispheres captures magnetosheath flux tubes at the dayside magnetopause [Onsager *et al.*, 2001; Walker *et al.*, 2003; Lavraud *et al.*, 2006b; Marcucci *et al.*, 2008]. The captured flux tubes are then convected into the tail [Song and Russell, 1992; Raeder *et al.*, 1995, 1997; Li *et al.*, 2005, 2008].

¹Space Science Center, University of New Hampshire, Durham, New Hampshire, USA.

²Space Sciences Laboratory, University of California, Berkeley, California, USA.

[7] 2. Diffusion processes facilitated by the Kelvin-Helmholtz instability allow magnetosheath plasma to diffuse across the boundary [Terasawa *et al.*, 1997; Fairfield *et al.*, 2000; Fujimoto and Terasawa, 1994; Nykyri and Otto, 2001; Nykyri *et al.*, 2006; Hasegawa *et al.*, 2004, 2006].

[8] On the basis of the double high-latitude reconnection mechanism, Li *et al.* [2008] comprehensively studied the solar wind entry into the magnetosphere under northward IMF conditions. They show that there is an entry window through which the solar wind plasma flows to the dayside boundary and convects tailward to form the CDPS in the near-tail.

[9] Most of the CDPS observations have been made in the nightside. However, there are numerous observations of a mixture of magnetosheath plasma and magnetospheric plasma in the low latitude boundary layer (LLBL) during northward IMF conditions [Paschmann *et al.*, 1990, 1993; Le *et al.*, 1994, 1996; Bauer *et al.*, 2001b; Onsager *et al.*, 2001; Bogdanova *et al.*, 2008]. In their 3-D global hybrid simulation, Lin and Wang [2006] show that, as a result of magnetic reconnection occurring in both the northern and southern hemispheres, a thick magnetopause boundary layer is formed because of the capture of magnetosheath ions on the newly closed field lines.

[10] Most recently, the THEMIS spacecraft observed a layer of long-lasting magnetosheath-like plasma in the dayside closed field region attached to the magnetopause [Øieroset *et al.*, 2008a]. The observations suggest that double high-latitude reconnection may cause the trapping of magnetosheath plasma on the nose of the magnetosphere. In this study, we use the global MHD magnetosphere model, Open Global Geospace Circulation Model (OpenGGCM), to simulate this event and further explore the relation between the double high-latitude reconnection and the formation of this layer of cold and dense plasma in the dayside magnetosphere.

2. Observations

[11] Since Øieroset *et al.* [2008a] have reported the observations on 3 June 2007 in detail, we only give a brief summary here. At 15:25 UT, the IMF near the Earth, deduced from ACE measurement, abruptly turned to dominantly duskward and then became increasingly more northward over the next 35 min, followed by one hour (16:00–17:00 UT) of relatively steady northward and dawnward IMF. The IMF became dominantly southward after 17:07 UT.

[12] From 15:22 UT, the five THEMIS spacecraft [Angelopoulos, 2008] traversed the region surrounding the magnetopause one after another from the magnetosphere to the magnetosheath, as shown in Figure 1. Before the IMF turned northward at 15:25 UT, the leading spacecraft THEMIS-B had already been in the magnetosheath, and the remaining four spacecraft (D, C, E, and A) were located inside the hot magnetosphere. Starting at 15:51 UT, all four spacecraft consecutively encountered magnetosheath-like plasma which was stagnant, with a stable magnetic field and heated magnetosheath ions and electrons. The field-aligned and anti-field-aligned electron fluxes that were well balanced at all energies indicate that the spacecraft was on closed field lines. Otherwise the hot magnetospheric electrons would simply stream out and be lost if the field line was not closed. The average densities observed by THEMIS

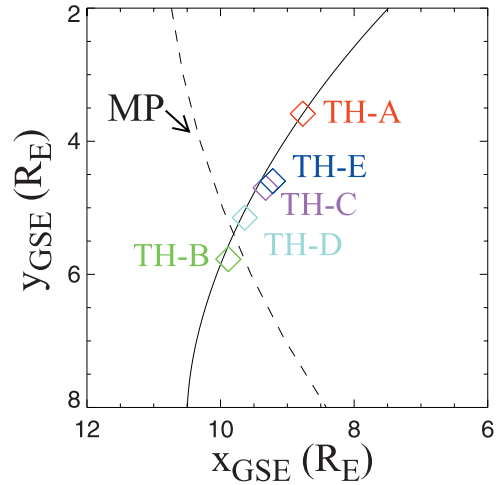


Figure 1. THEMIS orbit and spacecraft locations at the time when crossing the magnetopause and entering the magnetosheath on 3 June 2007.

D, C, E, and A are 4.6 , 5.6 , 6.7 , and 3.3 cm^{-3} , respectively, all of which are much higher than the density in the nightside CDPS. Combining all four spacecraft, this cold dense plasma layer (CDPL) was observed continuously from 15:51 UT (TH-D) to 17:05 UT (TH-A). Thus this CDPL was a persistent spatial region for over 74 min, during which the IMF was northward. The magnetosheath-sourced dayside CDPL appeared to become more mixed, with increasingly higher fluxes of hot magnetospheric ions and electrons as time progressed. This observed CDPL is attached to the magnetopause. The multiple spacecraft observations make it possible to estimate the CDPL thickness, which was found to be $1.1 R_E$ along the spacecraft track, or $\sim 0.9 R_E$ normal to the magnetopause at 16:30 UT near 13.5 MLT. THEMIS observed alternating sunward and tailward slow flows in the CDPL.

3. Simulation

[13] OpenGGCM solves the resistive MHD equations on a nonuniform rectilinear grid, with a minimum grid spacing at GSE $y = 0$ and $z = 0$ for the y and z directions, respectively, and at a point near the dayside magnetopause for the x direction. The outer boundary conditions on the dayside are the solar wind and IMF conditions, while those on the other five outer boundaries are free (i.e., normal derivatives vanish). The inner boundary conditions are derived from an ionospheric model coupling with the magnetosphere model. Field-aligned currents (FAC) are computed just outside a spherical region of radius $3.5 R_E$, centered around the Earth, and mapped to a spherical-polar ionosphere grid at $1 R_E$, using a dipole magnetic field model. The ionosphere potential is solved on the surface of a sphere with a $1.02 R_E$ radius. The ionospheric electric field is mapped back to the surface of the sphere with a $3.5 R_E$ radius. In an OpenGGCM simulation, the ionosphere can be modeled either simply as a sphere with constant uniform conductance, by empirical parameters [Robinson *et al.*, 1987], or by the NOAA Coupled Thermosphere Ionosphere Model (CTIM) [Fuller-Rowell *et al.*, 1996]. A more detailed

description of the OpenGGCM model and its ionosphere coupling can be found in related articles [Raeder *et al.*, 1998, 2001; Raeder, 2003; Raeder *et al.*, 2008].

[14] For this event, we use solar wind data from WIND spacecraft for the time period from 10:00 UT to 18:00 UT on 3 June 2007 to drive the simulation in a domain of GSE $(-24, 650) \times (-48, 48) \times (-48, 48)R_E$ with a minimum grid size of $0.12 R_E$ and about 28 million grid points. The CTIM is used as the coupled ionosphere model. The grid distribution in this simulation is designed to put emphasis on dayside and flanks and has high cost in computation. The parameter values of the whole domain are written out every 3 min. The values at a given position and a given time can be obtained from linear spatial and temporal interpolation for further analysis and tracing of fluid elements.

4. Simulation Versus Observation

[15] Figure 2 shows a comparison of THEMIS-C observations and the simulation results. From top to bottom, Figure 2 shows the plasma density, the temperature, the three magnetic field components, the flow speed, the azimuth flow direction, and the elevation flow direction; the bottom panel shows the clock angles for the IMF at position $(20,0,0)R_E$ in the simulation, the THEMIS-B magnetic field, and the THEMIS-B magnetic field in the simulation. All the vectors are in GSE coordinates. The black lines show the THEMIS measurements, and the red lines show the OpenGGCM results.

[16] The solar wind conditions in the simulation are taken from the WIND spacecraft, which was $\sim 251.2 R_E$ upstream of the Earth during this event, and thus are most likely different from the actual solar wind that hits the Earth. Since THEMIS-B was in the magnetosheath after $\sim 15:10$ UT, the time series of the magnetic field clock angle for THEMIS-B represents the actual variation of the IMF clock angle during this event. The solar wind conditions at GSE $(20,0,0)R_E$ in the simulation represent the solar wind conditions near the Earth in the simulation and near the WIND position $\sim 251.2 R_E$ upstream of the Earth with a lag of the time for the solar wind to travel from WIND to GSE $(20,0,0)R_E$. The bottom panel in Figure 2 indicates that the duskward IMF arrived at the magnetopause at about 15:35 UT in the simulation, considering that the time for the solar wind to flow from GSE $(20,0,0)R_E$ to GSE $(10,0,0)R_E$ is about 5 min. THEMIS-B was near the magnetopause at 15:25 UT, when it began to observe the duskward IMF. Thus the duskward IMF arrived at the magnetopause about 10 min later in the simulation than in reality. The northward IMF ended at around 17:25 UT in the simulation, while it ended at 17:10 UT in reality.

[17] The density time series, which is of primary interest here, is relatively well reproduced in the simulation. In the magnetosphere the observed density was low ($\sim 0.5 \text{ cm}^{-3}$) before THEMIS-C entered the CDPL at $\sim 15:50$ UT, and the simulation results are consistent with the observed values in this region. However, after 16:30 UT, when THEMIS-C entered the magnetosheath, the density in the simulation remains lower than the observed values. This discrepancy is most likely due to the lower solar wind density ($\sim 5.0 \text{ cm}^{-3}$) in the simulation, and the same level of solar wind speed in both the simulation and reality. During this event, the solar

wind density was higher (up to $\sim 10.0 \text{ cm}^{-3}$) at ACE than at WIND, and the solar wind speed at ACE was almost the same as that at WIND. The simulation misses the density drop and temperature jump around 17:30 UT, both of which are a result of a double crossing of the magnetopause that is not reproduced in the simulation, mainly because of a different solar wind conditions in the simulation.

[18] The magnetosphere temperature, shown in the second panel, is too low by an order of magnitude in the simulation because the OpenGGCM does not include a ring current. However, this is of minor consequence because the region has a low beta plasma, where the plasma pressure contributes little to the dynamics. In the CDPL and magnetosheath, the temperature is well reproduced with only a maximum difference of $\sim 0.2 \text{ keV}$.

[19] The magnetic field of the simulation follows the trend of the observed field fairly closely but misses the small-scale structures. In particular, none of the observed high-frequency fluctuations that are clearly visible in the magnetosheath and the CDPL are present in the simulation results. Also, some of the sharp field rotations in the magnetosheath in the data, especially the one representing the crossing of the magnetopause, are also missing in the simulation results. These results are to be expected, because the simulation cannot resolve fluctuation of this frequency, and the rotations are washed out first by the limited resolution and the diffusion in the code, and then by the linear interpolation of the values within the 3-min output time step. Another reason why the crossing of the magnetopause at 16:30 UT is not shown here is that the magnetic shear angle in the simulation is near zero when the virtual THEMIS-C crosses the magnetopause. At $\sim 16:30$ UT in the simulation, both the IMF and geomagnetic field clock angles near the magnetopause are near zero, and thus the field rotation is almost zero. The virtual THEMIS-B's magnetic field clock angle after $\sim 15:45$ UT shown in the bottom panel of Figure 2 indicates the value of the IMF clock angle near the magnetopause, and its value before 15:30 UT, when the virtual THEMIS-B is still inside the magnetopause, indicates the value of geomagnetic field clock angle which is fixed in the simulation. From $\sim 16:00$ UT to $\sim 16:30$ UT, the magnetosheath IMF clock angle is near zero in the simulation but becomes near -30 degrees after $\sim 16:40$ UT. As discussed before, the northward IMF arrives about 10 min later in the simulation than in reality and consequently causes the near-zero IMF clock angle near the magnetopause at 16:30 UT in the simulation. The 10-min time shift of the northward IMF in the simulation mainly causes the discrepancy in showing values along the orbit of the virtual satellites, but it should not change the main physical results due to northward IMF as long as the IMF behavior is similar in the simulation and in reality. In this event, from $\sim 16:00$ UT to $\sim 16:15$ UT in the observations and from $\sim 15:50$ UT to $\sim 16:10$ UT in the simulation, the IMF clock angle rotates from ~ 30 degrees to ~ -30 degrees and becomes near zero for some time. We will further discuss in section 5 how the IMF may affect the main findings in this study.

[20] Both in the data and in the simulation, the flow speed is nearly stagnant before entry into the magnetosheath, as shown in the speed panel of Figure 2. After entering the magnetosheath, the virtual flow speed is enhanced to the

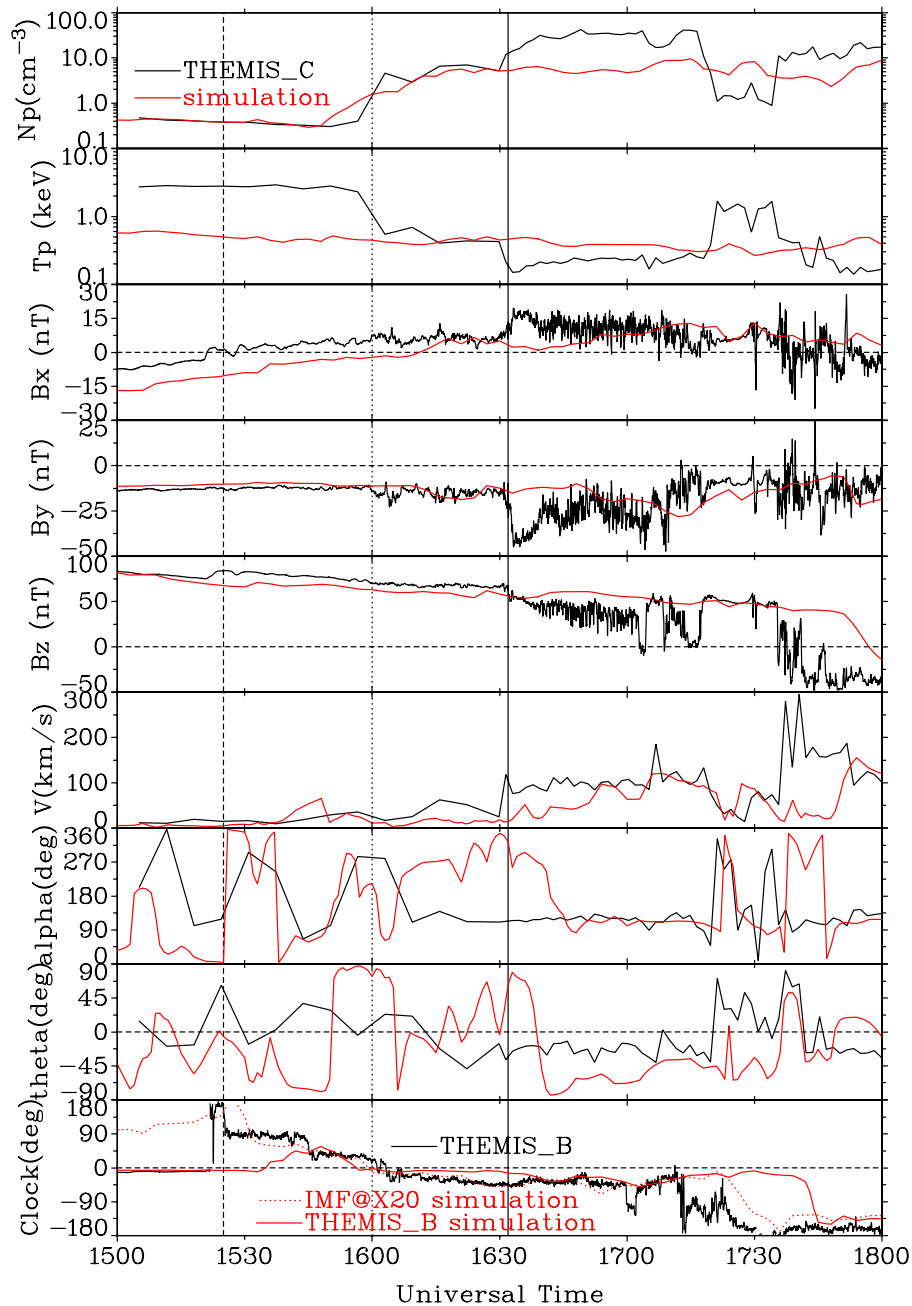


Figure 2. The comparison between the THEMIS-C observations and the corresponding simulation results for time period from 15:00 UT to 18:00 UT on 3 June 2007 when the spacecraft was flying outbound. From top to bottom, the panels are the plasma density, the plasma temperature, the magnetic field x component, the magnetic field y component, the magnetic field z component, the flow speed, the flow azimuth angle (0° for sunward direction), the flow elevation angle ($\text{atan}(V_z/|V_{xy}|)$), and the magnetic field clock angles (0° for pure northward direction) for THEMIS-B observation, THEMIS-B in the simulation, and IMF at $(20,0,0)R_E$ in the simulation. All the vectors are in GSE coordinates. The solid black lines are THEMIS observations, and the solid red lines are simulation results. The dashed vertical line indicates the arrival of the northward IMF, the dotted vertical line indicates the encountering of the cold dense plasma sheet, and the solid vertical line indicates the crossing of the magnetopause, all are based on the THEMIS observations.

same level as the observation and follows a similar trend of fluctuation. When in the magnetosphere, the flow is so slow that the flow direction is highly variable both in the data and in the simulation, and the comparison may not make any

sense. When in the magnetosheath, the azimuth flow direction of the simulation agrees very well with the observation, showing almost the same direction and similar fluctuation. In the simulation, the elevation angle indicates

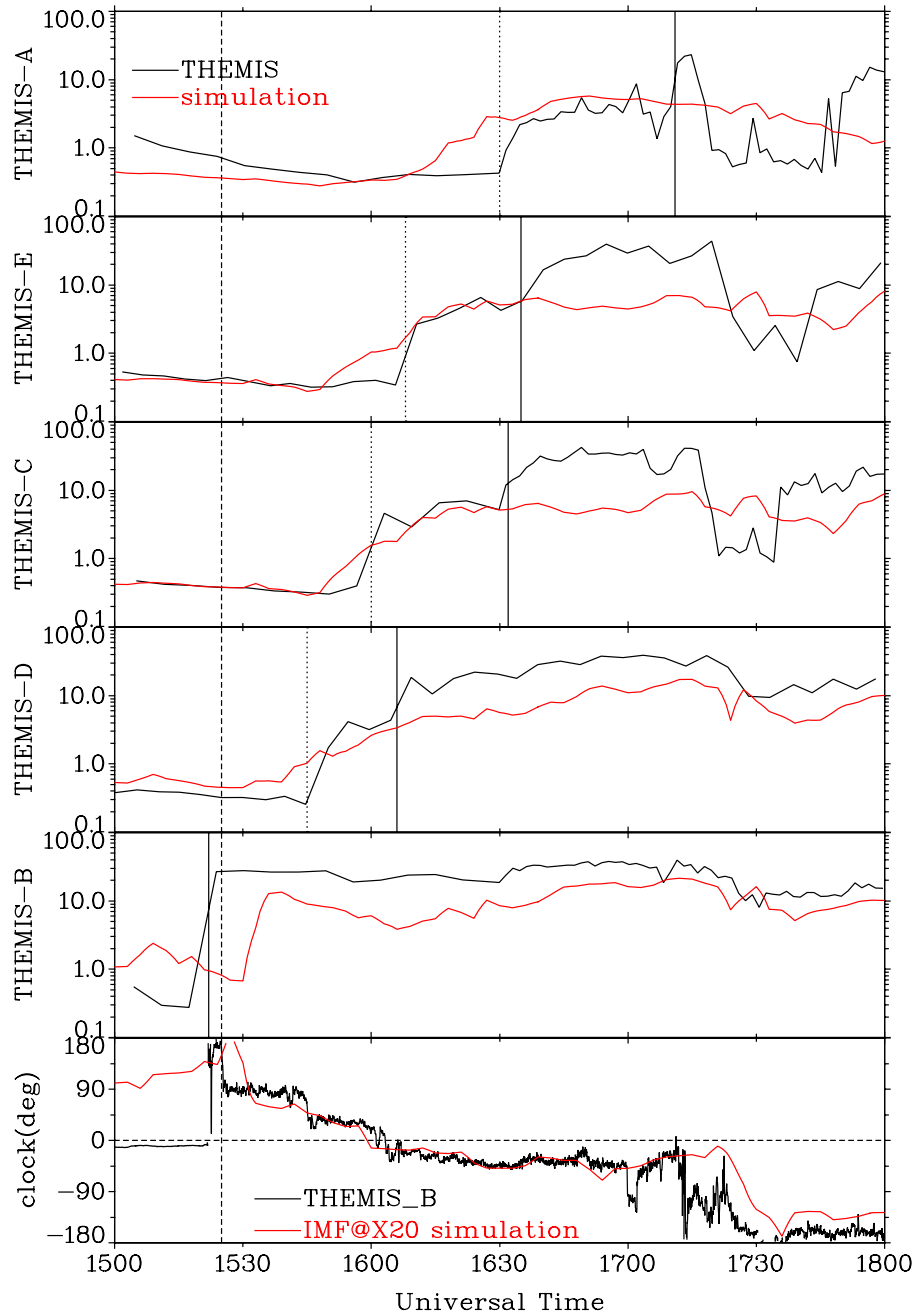


Figure 3. The comparison between the plasma densities measured by all five THEMIS spacecrafts and the corresponding simulation results. Shown from the top are plasma densities for THEMIS A, E, C, D, and B, in the position order from the magnetosphere to the magnetosheath. The bottom panel shows the magnetic field clock angles for THEMIS-B observation and IMF at $(20,0,0)R_E$ in the simulation. The vertical lines have the same meaning as those in Figure 2.

that the flow is more southward in the magnetosheath from $\sim 16:40$ UT to $\sim 17:20$ UT than the observed flow. The overall agreement on the flow direction in the magnetosheath gives us confidence that the simulation reproduces the correct physical process, because the plasma flows underlie the transport of plasma and field (via Faraday's law) and thus are the prime signatures of magnetospheric dynamics.

[21] In Figure 3 we compare the density time series at all five THEMIS spacecraft, showing both the observations and the simulation results. From top to bottom, the probes

are ordered by their position, with the one closest to the Earth (THEMIS-A) at the top. Overall, the simulation reproduces the density time series reasonably well. At the first four probes, the encounter of the CDPL in the simulation occurred too early by about 15 min for THEMIS-A and THEMIS-E, and by about 5 min for THEMIS-C and THEMIS-D. This discrepancy is mainly due to a wider CDPL with its inner boundary being closer to the Earth so that the virtual spacecraft in the simulation entered the layer earlier when it was flying outbound. The CDPL entry in the

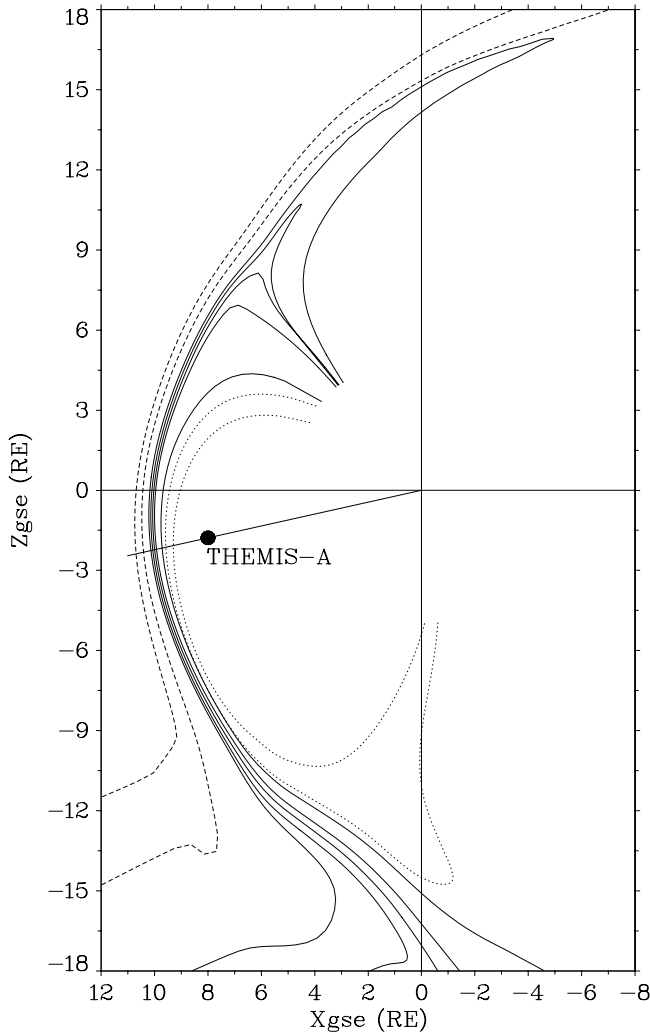


Figure 4. The GSE XZ projection of the magnetic field lines threading points on a radius line passing the THEMIS-A position at time 16:30 UT in the simulation. From left to right, the first two dashed lines are IMF field lines, the last two dotted lines are closed field lines, and the rest are open field lines.

simulation is less sharp. The smearing out of the CDPL entry discontinuity is most likely caused by numerical diffusion. As shown below, the thickness of the CDPL is of the order of $1-2 R_E$. Thus, the CDPL is only resolved by 10–20 grid cells in its smallest dimension. Such a thin layer will invariably diffuse in the simulation and thus become broader and less pronounced. THEMIS-B, the probe farthest away from the Earth, did not observe the CDPL because it was already in the magnetosheath before the arrival of northward IMF. The virtual THEMIS-B entered the magnetosheath about 10 min later than THEMIS-B in reality, mainly because the magnetopause was farther away from the Earth in the simulation and thus the virtual spacecraft stayed longer in the magnetosphere. In the simulation, the duskward IMF arrived with an enhancement of dynamic pressure, and compared to the observations it arrived 10 min late. Thus the magnetopause in the simulation was much farther away before THEMIS-B entered the magnetosheath

and became closer after the arrival of the duskward IMF. Therefore, the virtual THEMIS-B entered the magnetosheath later, but other virtual spacecraft could still enter the CDPL earlier because of the wider virtual CDPL and the less distant magnetopause. In spite of the discrepancy, and diffusion notwithstanding, the simulation shows the probes entering the CDPL in the observed order, thus again indicating that the simulation captures the correct physical processes.

5. Formation of Dayside CDPL

[22] The THEMIS observations clearly show that a CDPL with magnetosheath-like but stagnant plasma exists persistently and immediately earthward of the magnetopause during northward IMF conditions. As suggested by *Øieroset et al.* [2008a], local diffusion and Kelvin-Helmholtz instability are not likely to be important for the formation of the observed dayside CDPL. The presence of counter-streaming and heated magnetosheath electrons on CDPL field lines strongly indicates that the most likely formation mechanism is the capture of magnetosheath plasma by poleward-of-cusp reconnection in both hemispheres.

[23] The simulation results confirm this interpretation. Figure 4 shows the magnetic field lines threading through a radial line passing through THEMIS-A position at 16:30 UT when the IMF is northward. These field lines show the transition from IMF field lines to open field lines and finally to newly closed field lines. The kinked section of the field line near the cusp in either hemisphere indicates a newly reconnected field line as a result of poleward-of-cusp reconnection. Once a newly closed field line is created, some of the magnetosheath plasma is trapped into the dayside closed field region. The captured plasma thus has temperature and density which are intermediate between those of the magnetosheath and the magnetosphere. A boundary layer of magnetosheath plasma on closed field lines thus forms as long as the double high-latitude reconnection continuously occurs.

[24] The open field lines between the IMF field line and the closed field line also indicate that there is a boundary layer of magnetosheath plasma on open field lines. Although *Øieroset et al.* [2008a] did not report this structure in their paper, the authors checked the electron pitch angle data and did see evidence for an open field layer outside the magnetopause, but the data is in low resolution. *McFadden et al.* [2008] found such an open region near the low latitude boundary from THEMIS observations. They found the transition of sheath plasma with no electron heating to unidirectional heated electrons followed by bidirectional heated electrons, which is consistent with the field line topology shown in Figure 4. It should be kept in mind that these magnetic field lines in Figure 4 are not the same field lines frozen into the same traveling fluid element; i.e., it is a snapshot of field lines at different locations. Other MHD simulations also have shown a boundary structure composed of a closed boundary layer and an open boundary layer under northward IMF conditions [*Siscoe and Siebert, 2003; Li et al., 2008*].

[25] To find out how the magnetosheath plasma gets into the dayside magnetosphere and forms a layer of cold dense plasma in the simulation, we traced the fluid elements backward in time for 1.5 hours, starting from locations near

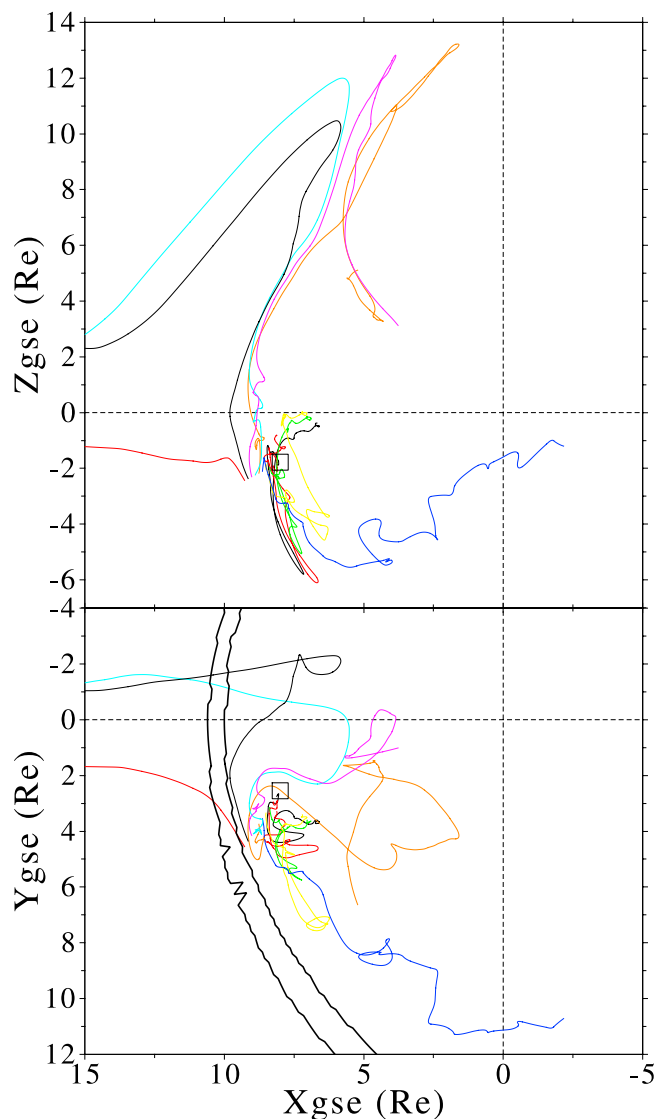


Figure 5. Paths of the fluid elements that arrive at points in the CDPL near the location of THEMIS-A, indicated by the small square, at 16:30 UT when it encounters the CDPL. The outer thick black line shows the IMF boundary, while the thick black line further earthward shows the boundary of the closed geomagnetic field, both at 16:30 UT. The paths are computed by backward tracing of the fluid elements for 1.5 hours.

the position ($GSE(7.99, 2.55, -1.78)R_E$) of THEMIS-A at 16:30 UT when it encountered the CDPL. The starting points locate on the line connecting THEMIS-A and THEMIS-C. Figure 5 shows the paths of these traced fluid elements arriving at the CDPL at 16:30 UT, and the boundaries among IMF, open field, and closed field on the equatorial plane at 16:30 UT. The black line, red line, and light blue line coming from sunward represent paths of fluid elements that flow from the magnetosheath and are captured by double high-latitude reconnection. With traced starting points closer to the Earth, the pink line and the orange line are the paths of fluid elements that originate from the magnetosphere. The dark blue line indicates a flow path coming from the tail flank region. However, this line may

not be real because it looks like a random walk for some places, and the computation of a flow path in a turbulent region using simulation data output in a relatively big time step (3 min in this simulation) is not dependable. The other paths show that some fluid elements flow southward and then turn northward, mainly within the CDPL. The flow is so stagnant within the CDPL that we could not trace these other paths out of the CDPL after 1.5 hours, which is the total tracing period. Although Figure 5 shows the possible sources (magnetosheath and magnetosphere) of the CDPL, it doesn't indicate which source is the dominant one. However, considering the tenuous magnetosphere and the dense magnetosheath, the only dominant source of the CDPL is the magnetosheath plasma.

[26] Figure 4 and the paths from the solar wind in Figure 5 show that a solar wind plasma fluid element directly

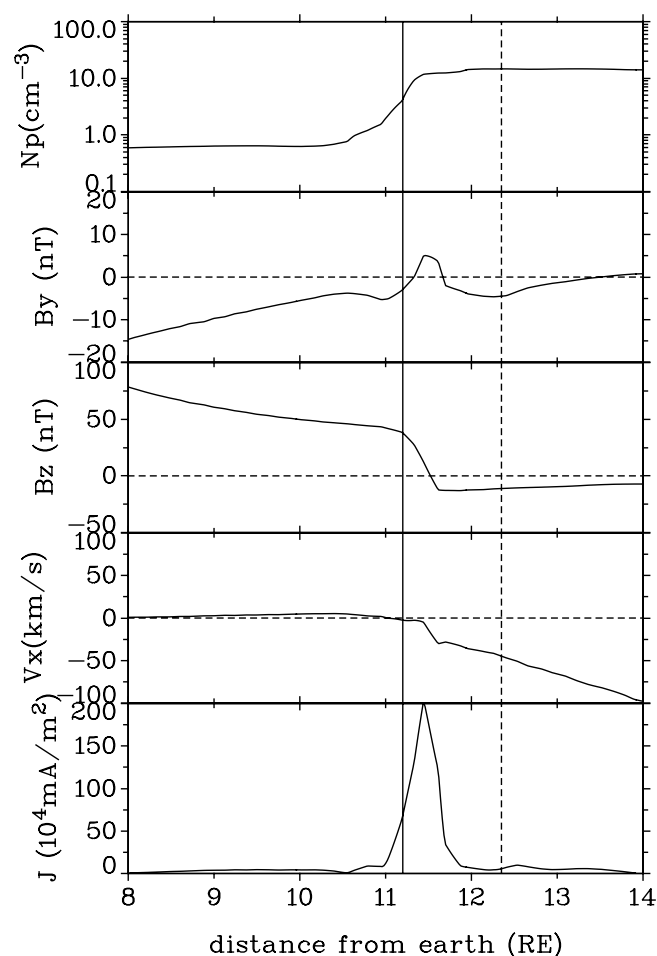


Figure 6. The simulation results at time 13:45 UT when the IMF was southward, and along the radius line passing through the position $GSE(8.06, 2.6, -1.8)R_E$ at which the THEMIS-C locates at 16:30 UT. Shown from top to bottom are plasma density, y component of magnetic field, z component of magnetic field, x component of velocity, and current density. All the vectors are in GSE coordinates. The vertical solid line indicates the boundary between the closed field region and the open field region. The vertical dashed line indicates the boundary between the open field region and the IMF field region.

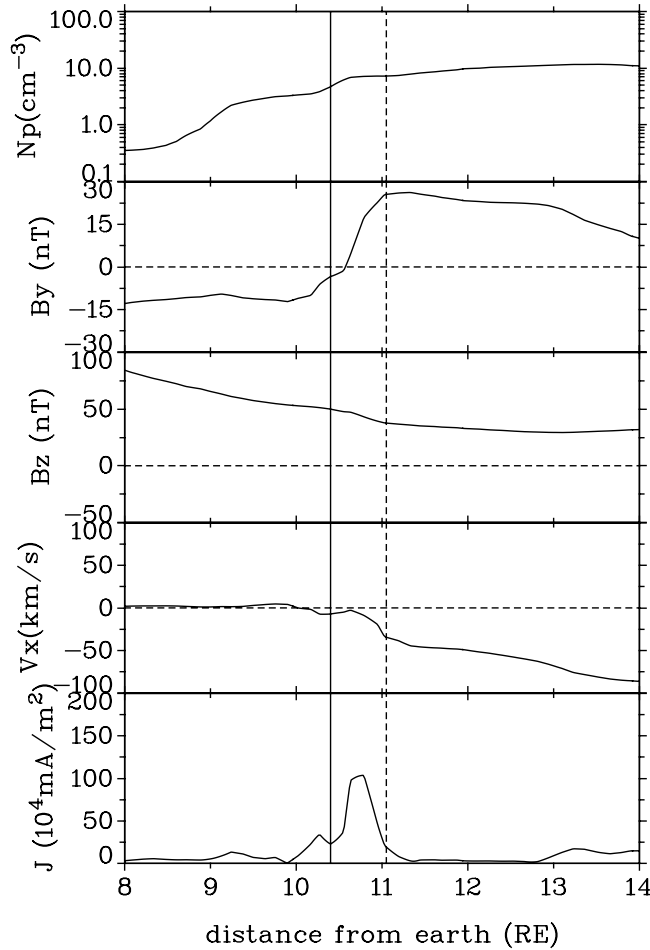


Figure 7. The same plot as Figure 6 except that the results are for the time 16:03 UT when the IMF is northward.

enters the closed field region from the magnetosheath crossing an open field region when its frozen-in magnetic field line changes from an IMF field line to an open field line, then finally to a closed field line. During this process, it comes across the magnetopause. Where is the magnetopause? In Figure 2, the in situ observations show clearly the time when THEMIS was crossing the magnetopause, but the virtual observations in the simulation are not due to the 3-min data output time step and low shear angle at the magnetopause. We plot the simulation results for every output time step (3 min) along a radial line passing through the position GSE(8.06,2.6,-1.8) R_E where THEMIS-C located at 16:30 UT. Figures 6–8 are three examples. Figure 6 is the plot of values at 13:45 UT when the IMF was southward. The magnetopause is clearly indicated by the peak of current density and the corresponding changes of V_x , B_y , B_z , and N_p . The solid vertical line indicates the boundary of the closed field (or inner boundary of the open field), and the dashed vertical line indicates the boundary of the IMF field (or the outer boundary of the open field). It seems that the magnetopause usually locates within the open field region when the IMF is southward. Figure 7 is the plot of values at 16:03 UT when the IMF was northward. The magnetopause is also clearly indicated by the peak of current density, which is much lower than that

during southward IMF, and the corresponding changes of V_x , B_y and N_p . The peak of current density is inside the open field region. Figure 8 is the plot of values at 16:30 UT when the IMF was northward and the shear angle was very small. For this situation, the current density is very low, and the magnetopause is difficult to determine. Examining all similar plots for the whole simulation, we found that the magnetopause (i.e., the current layer), can be clearly identified for high shear. The peak of the current layer most likely locates within the open layer for high shear. For low shear, the current density is very low and usually has several small peaks near the open layer. The current layer does not exactly coincide with the open layer because part of the current layer may be in the closed field region and/or in the IMF region. This boundary structure in the simulation agrees with what *Fuselier et al.* [1995] found in AMPTE/CCE observations in which the magnetosheath boundary layer (MSBL), which is the layer sunward of the magnetopause, is open, and the LLBL, which is the layer earthward of the magnetopause, is partially open.

[27] Figure 9 clearly shows a layer of dense plasma that is located on closed field region bordering the dayside magnetopause, which is almost within the open field region as indicated by Figure 7. It shows a bifurcating flow within the open field region and at the skin of the layer of cold dense

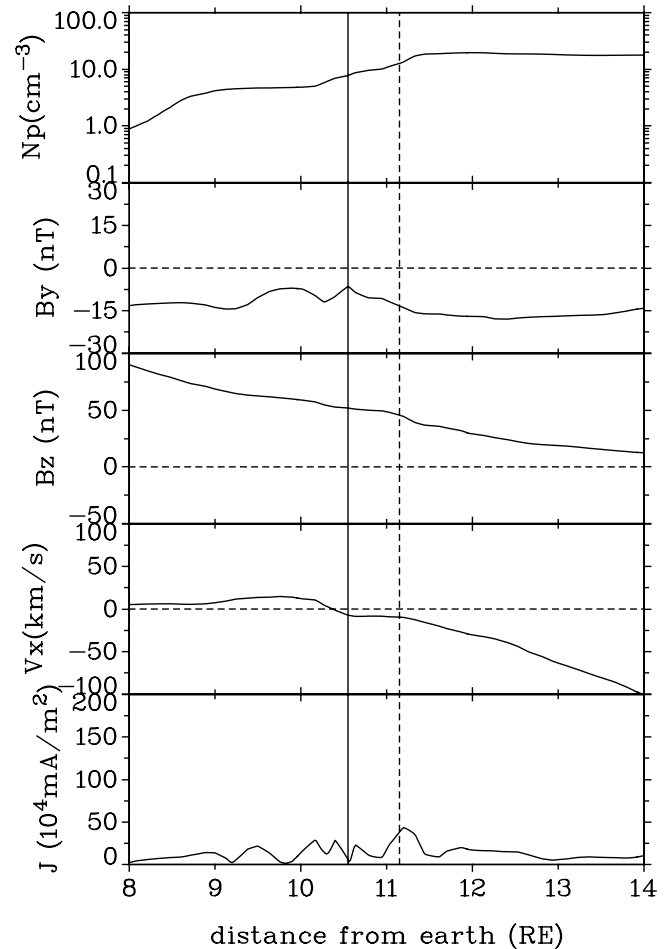


Figure 8. The same plot as Figure 6 except that the results are for the time 16:30 UT when the IMF is northward.

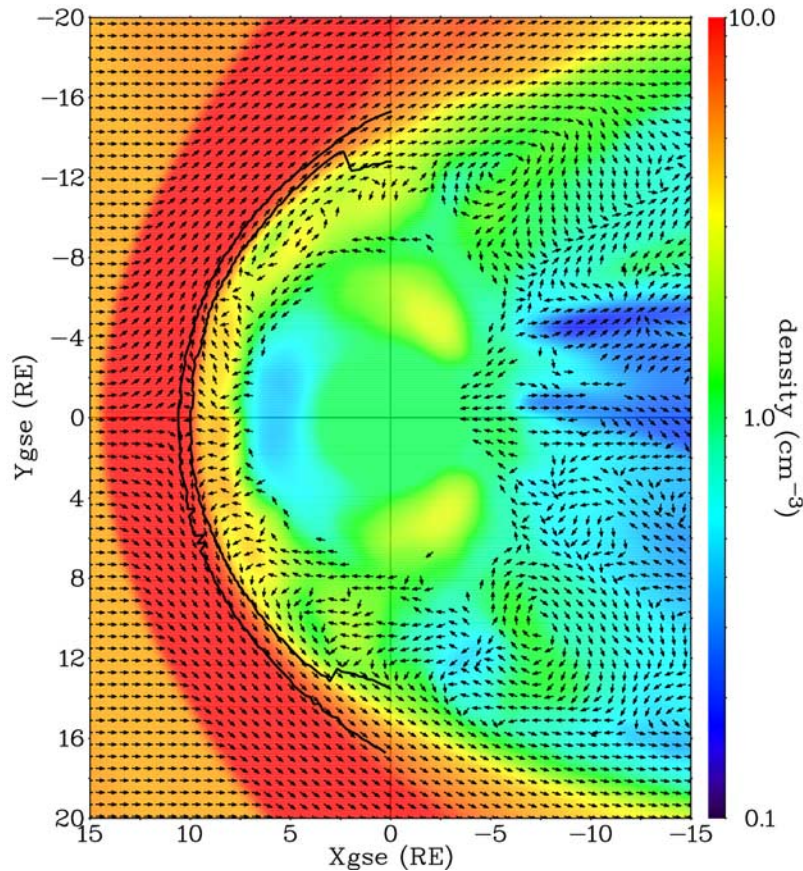


Figure 9. The plasma density and flow velocity field projected on GSE equatorial plane at time 16:30 UT in the simulation. The vectors are normalized to unit vectors to represent the flow directions projected on the equatorial plane. Vectors with velocity magnitude on the plane less than 5 km/s are not shown. The outer thick black line shows the boundary between the IMF and the open field, while the thick black line further earthward shows the boundary between the dayside closed field and the open field.

plasma, which is immediately earthward of the closed boundary. However, the dense plasma farther earthward shows a different flow direction, which is sunward and toward the noon region.

[28] Figure 10 shows that the region including the open field layer and the skin of the dayside CDPL has a significant difference in flow direction from either the magnetosheath or the earthward part of the dayside CDPL. This region has a significant southward flow while its neighboring magnetosheath has a northward flow on the equatorial plane, and its neighboring earthward part of the CDPL has almost zero flow speed.

[29] This southward flow layer is further illustrated in Figure 11, which shows the color-coded north–south flow component on the noon–midnight meridian plane, the unity vectors for flow velocity projected on the plane, the closed field boundary, and the IMF field boundary on the plane in the dayside. In Figure 11, the closed boundary outlines the northern cusp region and indicates that the Earth’s dipole is tilted toward the Sun in the northern hemisphere at 16:30 UT. In the northern cusp region, there is a bifurcating flow indicating the cusp reconnection site. There is also a conjugate reconnection site at the southern cusp indicated

by the southern circle in Figure 11, but with a slower bifurcating flow.

[30] Figure 4 shows that open field lines extend from the northern cusp toward the south. *Lavraud et al.* [2005b] showed that an IMF flux tube will first participate in high-latitude reconnection at the northern (southern) hemisphere, and then at the southern (northern) hemisphere, when the geomagnetic dipole tilts sunward (antisunward) in the northern hemisphere, even for IMF with a nonzero x component. Thus, the open field lines will extend from the northern cusp toward the south and drape over the magnetopause for a geomagnetic dipole tilting sunward in the northern hemisphere. As indicated by the closed field boundary in Figure 11, the dipole tilts sunward in the northern hemisphere during this event. *Li et al.* [2008] also showed a layer of open field lines extending from the north cusp for the sunward tilted dipole in northern hemisphere in their MHD simulations with similar conditions.

[31] When the solar wind flows to the subsolar point, the flow is normally diverted around the magnetopause into northward flow and southward flow, as well as dawnward flow and duskward flow. The flow is nearly stagnant at the subsolar region and becomes faster as it flows tailward. The

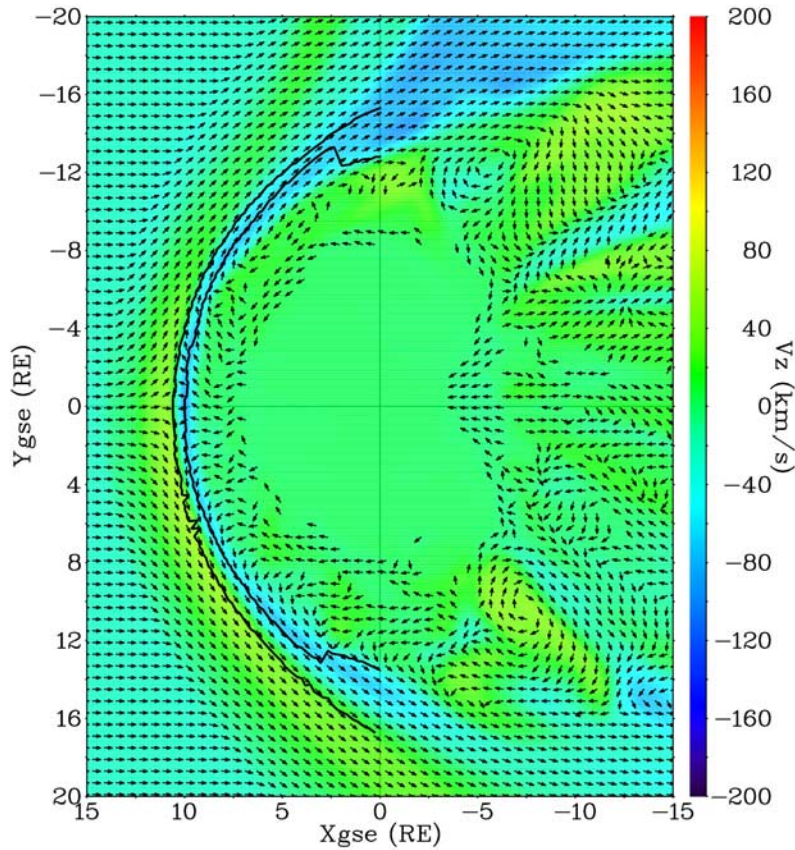


Figure 10. The same as Figure 9 except that the color represents the plasma flow GSE Z component.

northern part of the open layer should have a northward flow direction since it is mainly composed of magnetosheath plasma. However, in this case it has a systematically southward flow which is caused by the reconnection occurring at the northern cusp and the magnetic curvature force at the northern part of the open field. For the southern part of the open layer, the flow is southward as normal and no reconnection occurs on the open side. Therefore, the whole open layer has a southward flow. We found that this southward flow in the open layer lasts from $\sim 16:03$ UT to $\sim 17:10$ UT in the simulation, i.e., during the period of northward IMF. Examining the observed flow velocity as THEMIS entered the magnetopause, we found that the velocity was southward on average. However, THEMIS was in the southern hemisphere; therefore, THEMIS did not observe the southward flow in the northern part of the open layer. A superposed epoch analysis of seven IRM magnetopause crossings with low magnetic shear reported by *Bauer et al.* [2001b] shows that the flow in the boundary layer is generally directed toward high latitudes. However, the report of the event on 17 September 1984, which is from the same IRM data set but is presented in another paper [*Bauer et al.*, 2001a], shows equatorward flow on average in the Outer Boundary Layer, which is open in this event. Since the IRM spacecraft was on the GSE equatorial plane, this event cannot confirm the southward flow in the open layer. A statistical study of the flow when the spacecraft passes through the northern magnetopause under conditions of northward IMF and sunward tilted dipole in the northern

hemisphere will determine the existence of this open layer with southward plasma flow.

[32] Since the open layer has a southward flow in this event, the thin layer immediately earthward of this layer, i.e., the skin of the closed field boundary, will also have a slow southward flow because the field lines in the skin of the closed field were previously open field lines in the open layer. Therefore, the newly captured magnetosheath plasma flows southward, earthward, and duskward (or downward) tangentially into the skin of the CDPL. Once it enters the inner part of the CDPL, the flow becomes more stagnant and more turbulent. Figure 9 shows, at 16:30 UT, that most of dayside magnetospheric plasma near the CDPL flows sunward toward the noon region from dawnside or duskside of the magnetosphere. Examining other figures like Figure 9 but derived from other times, we found that sometimes the earthward tangential flow is dominant in the CDPL; sometimes the sunward and noonward flow is dominant, and sometimes they are mixed turbulently. Such flow behavior can explain why the THEMIS spacecraft did not observe a consistent tangential flow direction in the CDPL region (see the bottom panel of Figure 2 in the work of *Øieroset et al.* [2008a]).

[33] Although both observations and simulation suggest that Kelvin-Helmholtz instability is not likely to contribute to the formation of the dayside CDPL directly, there is still possibility that it occurs in the tail flanks and facilitates the mixing of the newly captured magnetosheath plasma, and/or even the mixing of the magnetosheath plasma directly into

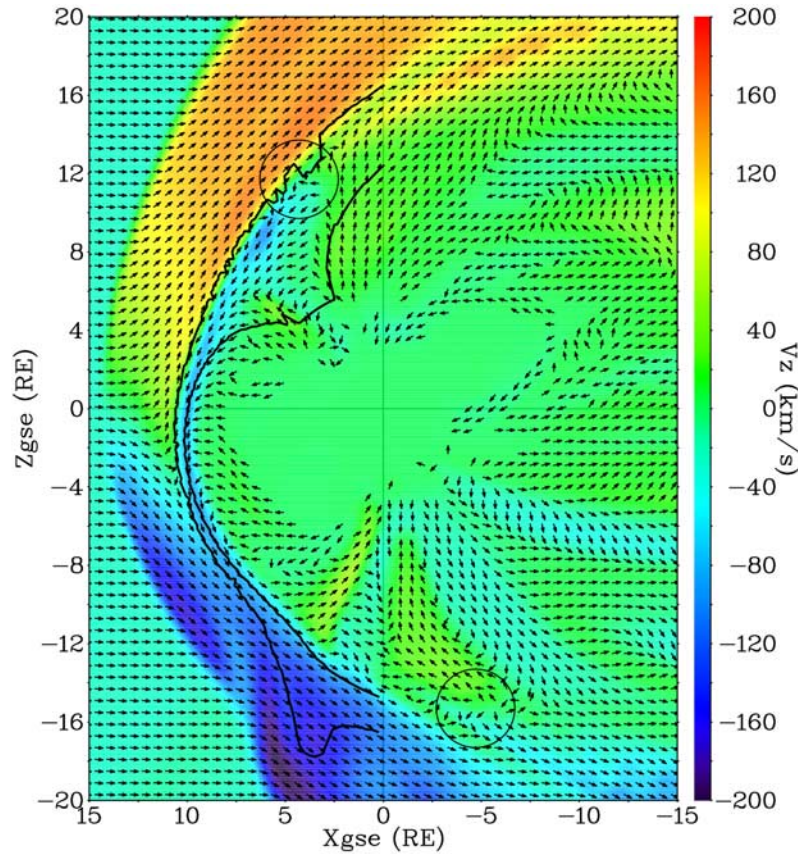


Figure 11. The same as Figure 10 except that the values are shown on the GSE noon-midnight meridian plane. The two circles indicate two bifurcating flow regions near the northern cusp and southern cusp.

the magnetosphere. Some of the KHI-mix plasma may then convect toward the noon to contribute to the dayside CDPS.

[34] The thickness of this layer of cold dense plasma is near $2.0 R_E$ at time 16:30 UT on the equatorial plane as estimated from the yellow region shown in Figure 9. For comparison, Figure 12 shows no dense plasma inside the closed field region for the time of southward IMF conditions at 14:30 UT. We found that the thickness in the simulation grows at the beginning of northward IMF conditions and stays rather stable except for small variations in response to the change of solar wind conditions and different local time and latitude locations. The whole dayside CDPL in the simulation, as well as the dayside closed boundary, has a small motion corresponding to the solar wind dynamic pressure. The THEMIS estimation of the thickness is $\sim 0.9 R_E$ at time 16:30 UT for the location near GSE $(7.99, 2.55, -1.78)R_E$. The thickness difference between the observation and the simulation is mainly due to the numerical diffusion in the simulation. We ran another simulation with higher resolution in the x direction and found that the CDPL thickness is about $1.1 R_E$. Since numerical diffusion tends to smear out jump boundary conditions, and greater grid size in the x direction will cause greater diffusion in the x direction, the dayside CDPL, whose density is one order of magnitude greater than that in the magnetosphere, is thus thicker for greater grid size in the x direction. The numerical magnetic diffusion may also increase the high-latitude reconnection rate and cause more magnetosheath plasma to be captured. However, the numer-

ical magnetic diffusion is not likely important [Raeder, 1999]. Even though the reconnection rate is increased and more magnetosheath plasma is captured, it does not necessarily result in thicker CDPL, because the captured plasma may spread away toward the nightside.

[35] Figures 4 and 5 indicate that the magnetosheath plasma directly enters the magnetosphere after it was captured. Observations have indicated that the magnetosheath plasma convects directly across the magnetopause under low magnetic-shear condition [Fuselier *et al.*, 1995]. Such directly entering of magnetosheath plasma implies that the CDPL is formed rapidly after the northward turning of IMF. The THEMIS-B IMF clock angle shown in the bottom panel of Figure 3 indicates that the IMF was turning from southward to duskward and slightly northward at $\sim 15:25$ UT. The THEMIS-D density time series in Figure 3 shows that the CDPL was first detected at $\sim 15:45$ UT. Thus it took at most 20 min to form the CDPL. From 15:25 UT to 15:45 UT, the IMF is mainly duskward and slightly northward, but it can still cause the magnetosheath plasma to be captured and form the CDPL. Li *et al.* [2008] show that even a dawn-dusk-oriented IMF can cause significant solar wind plasma to enter the magnetosphere. The IMF clock angle at GSE $(20, 0, 0)R_E$ and the virtual THEMIS-D density in the simulation indicate that the time to form the CDPL is at most 10 min in the simulation.

[36] The solar wind and IMF were measured at the WIND spacecraft position, which was about $250 R_E$ upstream of the Earth during this event. Therefore, the simulation input

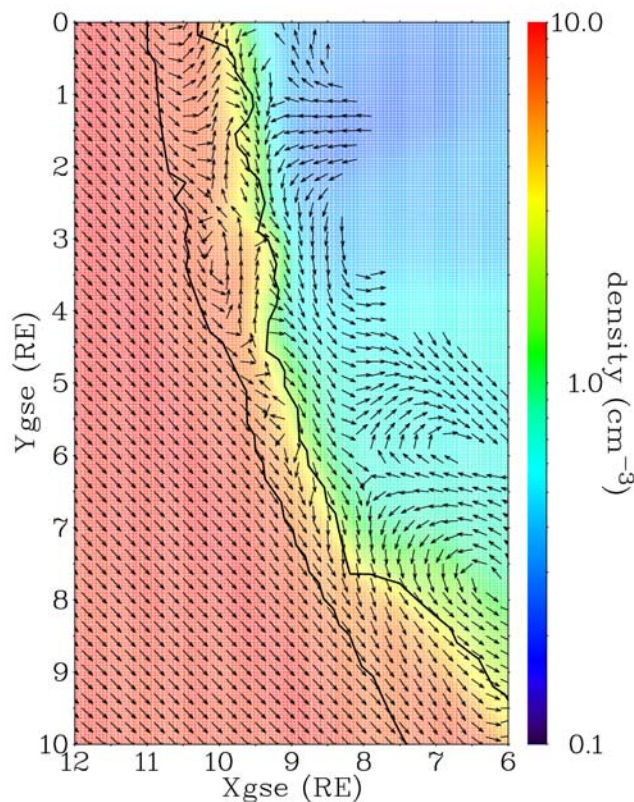


Figure 12. The same as Figure 9 except for smaller region and a different time at 14:30 UT when the IMF is southward.

data is most likely different from the data of the solar wind and IMF that actually hit the Earth. Now the question is whether some of the findings in this study would change if the simulation had given the correct magnetosheath magnetic field. From our OpenGGCM simulations run for this event and other real or artificial northward IMF events, we can always find the double high-latitude reconnection process, the CDPS, the CDPL, and the open layer. A change of the northward IMF may change the thickness and density of the CDPL, the thickness of the open layer, and the magnitude and direction of the open layer flow, which is also determined by the dipole orientation. However, how the properties of the CDPL, the open layer, and its flow change with various IMF, solar wind, and geomagnetic dipole conditions may need further event and simulation studies to find out.

6. Summary

[37] On 3 June 2007, THEMIS satellites observed a persistent layer of magnetosheath-like and nearly stagnant plasma immediately earthward of the dayside magnetopause [Øieroset *et al.*, 2008a]. The multisatellite observations established that this is a spatial structure adjacent to the magnetopause during the period of northward IMF conditions. The presence of counter-streaming and heated magnetosheath electrons during the crossing of this layer of cold dense plasma indicates the occurrence of double high-latitude reconnection, i.e., poleward-of-cusp reconnection in both hemispheres.

[38] We have successfully reproduced the observed day-side CDPL in the simulation for this event using global MHD magnetosphere model OpenGGCM. The simulation results reveal the mechanism of the formation of the dayside CDPL. In addition to the magnetospheric plasma, most of the plasma in the CDPL originates from the magnetosheath plasma that is captured by the double high-latitude reconnection under northward IMF conditions. The double high-latitude reconnection causes the formation of a closed boundary layer with the captured magnetosheath plasma. An open field layer is also formed between the magnetosheath IMF and the dayside closed field as a result of the high-latitude reconnection that first occurs at the northern cusp and then at the southern cusp for a reconnecting IMF field line. In the present event, the geomagnetic dipole tilting sunward in northern hemisphere and the reconnection at the northern cusp result in a southward flow within the open layer. The newly captured magnetosheath plasma thus flows southward and earthward tangentially across the magnetopause into the CDPL. Future statistical analysis under spacecraft observations of magnetopause crossing under northward IMF conditions will help to determine whether this feature is realistic.

[39] **Acknowledgments.** We acknowledge NASA contract NAS5-02099 and V. Angelopoulos for use of data from the THEMIS mission. Specifically, we acknowledge C. W. Carlson and J. P. McFadden for use of ESA data, K. H. Glassmeier, U. Auster and W. Baumjohann for the use of FGM data provided under the lead of the Technical University of Braunschweig and with financial support through the German Ministry for Economy and Technology and the German Center for Aviation and Space (DLR) under contract 50 OC 0302. We also acknowledge ACE, WIND and CDAWeb for the solar wind data. The work was supported by grant ATM-0503189 from the National Science Foundation GEM program, and by NASA grant SECIG P04-0025-O171. Computations were performed on the Zaphod Beowulf cluster which was in part funded by the Major Research Instrumentation program of the National Science Foundation under grant ATM-0420905.

[40] Wolfgang Baumjohann thanks Goetz Paschmann and another reviewer for their assistance in evaluating this paper.

References

- Angelopoulos, V. (2008), The THEMIS mission, *Space Sci. Rev.*, doi:10.1007/s11214-008-9336-1.
- Axford, W. I., and C. O. Hines (1961), A unifying theory of high latitude geophysical phenomena and geomagnetic storms, *Can. J. Phys.*, *39*, 1433.
- Bauer, T. M., G. Paschmann, N. Sckopke, R. A. Treumann, W. Baumjohann, and T.-D. Phan (2001a), Fluid and particle signatures of dayside reconnection, *Ann. Geophys.*, *19*, 1045.
- Bauer, T. M., R. A. Treumann, and W. Baumjohann (2001b), Investigation of the outer and inner low-latitude boundary layers, *Ann. Geophys.*, *19*, 1065.
- Baumjohann, W., G. Paschmann, and C. A. Cattell (1989), Average plasma properties in the central plasma sheet, *J. Geophys. Res.*, *94*, 6597.
- Bogdanova, Y. V., et al. (2008), Formation of the low-latitude boundary layer and cusp under the northward IMF: Simultaneous observations by Cluster and Double Star, *J. Geophys. Res.*, *113*, A07S07, doi:10.1029/2007JA012762.
- Borovsky, J. E., M. F. Thomsen, and D. J. McComas (1997), The superdense plasma sheet: plasmaspheric origin, solar wind origin, or ionospheric origin?, *J. Geophys. Res.*, *102*, 22,089.
- Denton, M. H., J. E. Borovsky, R. M. Skoug, M. F. Thomsen, B. Lavraud, M. G. Henderson, R. L. McPherron, J. C. Zhang, and M. W. Liemohn (2006), Geomagnetic storms driven by ICME- and CIR-dominated solar wind, *J. Geophys. Res.*, *111*, A07S07, doi:10.1029/2005JA011436.
- Fairfield, D. H., R. P. Lepping, E. W. Hones, S. J. Bame, and J. R. Asbridge (1981), Simultaneous measurements of magnetotail dynamics by IMP spacecraft, *J. Geophys. Res.*, *86*, 1396.
- Fairfield, D. H., A. Otto, T. Mukai, S. Kokubun, R. P. Lepping, J. T. Steinberg, A. J. Lazarus, and T. Yamamoto (2000), Geotail observations of the Kelvin-Helmholtz instability at the equatorial magnetotail boundary for parallel northward fields, *J. Geophys. Res.*, *105*, 21,159.

- Fujimoto, M., and T. Terasawa (1994), Anomalous ion mixing within an MHD scale Kelvin-Helmholtz vortex, *J. Geophys. Res.*, *99*, 8601.
- Fujimoto, M., A. Nishida, T. Mukai, Y. Saito, T. Yamamoto, and S. Kokubun (1996), Plasma entry from the flanks of the near-Earth magnetotail: Geotail observations in the dawnside LLBL and the plasma sheet, *J. Geomagn. Geoelectr.*, *48*, 711.
- Fujimoto, M., T. Terasawa, T. Mukai, Y. Saito, T. Yamamoto, and S. Kokubun (1998), Plasma entry from the flanks of the near-Earth magnetotail: Geotail observations, *J. Geophys. Res.*, *103*, 4391.
- Fuller-Rowell, T. J., D. Rees, S. Quegan, R. J. Moffett, M. V. Codrescu, and G. H. Millward (1996), A coupled thermosphere-ionosphere model (CTIM), in *STEP Report*, edited by R. W. Schunk, p. 217, Sci. Committee on Sol. Terr. Phys. (SCOSTEP), Natl. Oceanic and Atmos. Admin., Boulder, Colo.
- Fuselier, S. A., B. J. Anderson, and T. G. Onsager (1995), Particle signatures of magnetic topology at the magnetopause: AMPTE/CCE observations, *J. Geophys. Res.*, *100*, 11,805.
- Fuselier, S. A., R. C. Elphic, and J. T. Gosling (1999), Composition measurements in the dusk flank magnetosphere, *J. Geophys. Res.*, *104*, 4515, doi:10.1029/1998JA900137.
- Hasegawa, H., M. Fujimoto, T. D. Phan, H. Rème, A. Balogh, M. W. Dunlop, C. Hashimoto, and R. TanDokoro (2004), Transport of solar wind into Earth's magnetosphere through rolled-up Kelvin-Helmholtz vortices, *Nature*, *430*, 755.
- Hasegawa, H., M. Fujimoto, K. Takagi, Y. Saito, T. Mukai, and H. Rème (2006), Single-spacecraft detection of rolled-up Kelvin-Helmholtz vortices at the flank magnetopause, *J. Geophys. Res.*, *111*, A09203, doi:10.1029/2006JA011728.
- Hultqvist, B., M. Andre, S. P. Christon, G. Paschmann, and D. G. Sibeck (1999), Contributions of different source and loss processes to the plasma content of the magnetosphere, *Space Sci. Rev.*, *88*, 1–2, 355.
- Lavraud, B., M. H. Denton, M. F. Thomsen, J. E. Borovsky, and R. H. W. Friedel (2005a), Superposed epoch analysis of dense plasma access to geosynchronous orbit, *Ann. Geophys.*, *23*, 2519.
- Lavraud, B., M. F. Thomsen, M. G. G. T. Taylor, Y. L. Wang, T. D. Phan, S. J. Schwartz, R. C. Elphic, A. Fazakerley, H. Rème, and A. Balogh (2005b), Characteristics of the magnetosheath electron boundary layer under northward interplanetary magnetic field: Implications for high-latitude reconnection, *J. Geophys. Res.*, *110*, A06209, doi:10.1029/2004JA010808.
- Lavraud, B., M. F. Thomsen, J. E. Borovsky, M. H. Denton, and T. I. Pulkkinen (2006a), Magnetosphere preconditioning under northward IMF: Evidence from the study of coronal mass ejection and corotating interaction region geoeffectiveness, *J. Geophys. Res.*, *111*, A09208, doi:10.1029/2005JA011566.
- Lavraud, B., M. F. Thomsen, B. Lefebvre, S. J. Schwartz, K. Seki, T. D. Phan, Y. L. Wang, A. Fazakerley, H. Rème, and A. Balogh (2006b), Evidence for newly closed magnetosheath field lines at the dayside magnetopause under northward IMF, *J. Geophys. Res.*, *111*, A05211, doi:10.1029/2005JA011266.
- Lavraud, B., M. F. Thomsen, S. Wing, M. Fujimoto, M. H. Denton, J. E. Borovsky, A. Aanes, K. Seki, and J. M. Weygand (2006c), Observation of two distinct cold, dense ion populations at geosynchronous orbit: Local time asymmetry, solar wind dependence and origin, *Ann. Geophys.*, *24*, 3451.
- Le, G., C. T. Russell, and J. T. Gosling (1994), Structure of the magnetopause for low Mach number and strongly northward interplanetary magnetic field, *J. Geophys. Res.*, *99*, 23,723.
- Le, G., C. T. Russell, J. T. Gosling, and M. F. Thomsen (1996), ISEE observations of lowlatitude boundary layer for northward interplanetary magnetic field: Implications for cusp reconnection, *J. Geophys. Res.*, *101*, 27,239.
- LeMaire, J. (1977), Impulsive penetration of filamentary plasma elements into the magnetospheres of the Earth and Jupiter, *Planet. Space Sci.*, *25*, 887.
- Lennartsson, W. (1992), A scenario for solar wind penetration of Earth's magnetic tail based on ion composition data from the ISEE 1 spacecraft, *J. Geophys. Res.*, *97*, 19,221.
- Lennartsson, W., and E. G. Shelley (1986), Survey of 0.1 to 16 keV/e plasma sheet ion composition, *J. Geophys. Res.*, *91*, 3061.
- Li, W., J. Raeder, J. Dorelli, M. Øieroset, and T. D. Phan (2005), Plasma sheet formation during long period of northward IMF, *Geophys. Res. Lett.*, *32*, L12S08, doi:10.1029/2004GL021524.
- Li, W., J. Raeder, M. F. Thomsen, and B. Lavraud (2008), Solar wind plasma entry into the magnetosphere under northward IMF conditions, *J. Geophys. Res.*, *113*, A04204, doi:10.1029/2007JA012604.
- Liemohn, M. W., J.-C. Zhang, M. F. Thomsen, J. E. Borovsky, J. U. Kozyra, and R. Ilie (2008), Plasma properties of superstorms at geosynchronous orbit: How different are they?, *Geophys. Res. Lett.*, *35*, L06S06, doi:10.1029/2007GL031717.
- Lin, Y., and X. Y. Wang (2006), Formation of dayside low-latitude boundary layer under northward interplanetary magnetic field, *Geophys. Res. Lett.*, *33*, L21104, doi:10.1029/2006GL027736.
- Marcucci, M. F., I. Coco, D. Ambrosino, E. Amata, S. E. Milan, M. B. B. Cattaneo, and A. Retinò (2008), Extended SuperDARN and IMAGE observations for northward IMF: Evidence for dual lobe reconnection, *J. Geophys. Res.*, *113*, A02204, doi:10.1029/2007JA012466.
- McFadden, J. P., T. D. Phan, C. W. Carlson, V. Angelopoulos, K.-H. Glassmeier, and U. Auster (2008), Structure of the subsolar magnetopause regions during northward IMF: first results from THEMIS, *Geophys. Res. Lett.*, *35*, L17S09, doi:10.1029/2008GL033630.
- Nagata, D., S. Machida, S. Ohtani, Y. Saito, and T. Mukai (2007), Solar wind control of plasma number density in the near-Earth plasma sheet, *J. Geophys. Res.*, *112*, A09204, doi:10.1029/2007JA012284.
- Nishino, M. N., M. Fujimoto, G. Ueno, K. Maezawa, T. Mukai, and Y. Saito (2007a), Geotail observations of two-component protons in the midnight plasma sheet, *Ann. Geophys.*, *25*, 2229.
- Nishino, M. N., M. Fujimoto, G. Ueno, T. Mukai, and Y. Saito (2007b), Origin of temperature anisotropies in the cold plasma sheet: Geotail observations around the Kelvin-Helmholtz vortices, *Ann. Geophys.*, *25*, 2069.
- Nykyri, K., and A. Otto (2001), Plasma transport at the magnetospheric boundary due to reconnection in Kelvin-Helmholtz vortices, *Geophys. Res. Lett.*, *28*, 3565.
- Nykyri, K., A. Otto, B. Lavraud, C. Moukik, L. M. Kistler, A. Balogh, and H. Rème (2006), Cluster observations of reconnection due to the Kelvin-Helmholtz instability at the dawnside magnetospheric flank, *Ann. Geophys.*, *24*, 2619.
- Øieroset, M., M. Yamauchi, L. Liska, and B. Hultqvist (1999), Energetic ion outflow from the dayside ionosphere: Categorization, classification, and statistical study, *J. Geophys. Res.*, *104*, 24,915.
- Øieroset, M., T. D. Phan, M. Fujimoto, L. Chan, R. P. Lin, and R. Skoug (2002), Spatial and temporal variations of the cold dense plasma sheet: Evidence for a low-latitude boundary layer source?, in *Earth's Low-Latitude Boundary Layer*, *Geophys. Monogr. Ser.*, vol. 133, edited by P. T. Newell and T. G. Onsager, doi:10.1029/133GM25, AGU, Washington, D. C.
- Øieroset, M., J. Raeder, T. D. Phan, S. Wing, J. P. McFadden, W. Li, M. Fujimoto, H. Rème, and A. Balogh (2005), Global cooling and densification of the plasma sheet during an extended period of purely northward IMF on October 22–24, 2003, *Geophys. Res. Lett.*, *32*, L12S07, doi:10.1029/2004GL021523.
- Øieroset, M., T. D. Phan, V. Angelopoulos, J. P. Eastwood, J. P. McFadden, D. Larson, C. W. Carlson, K. H. Glassmeier, M. Fujimoto, and J. Raeder (2008a), THEMIS multispacecraft observations of magnetosheath plasma penetration deep into the dayside low-latitude magnetosphere for northward and strong B_y IMF, *Geophys. Res. Lett.*, *35*, L17S11, doi:10.1029/2008GL033661.
- Øieroset, M., T. D. Phan, D. H. Fairfield, J. Raeder, J. T. Gosling, J. F. Drake, and R. P. Lin (2008b), The existence and properties of the distant magnetotail during 32 hours of strongly northward interplanetary magnetic field, *J. Geophys. Res.*, *113*, A04206, doi:10.1029/2007JA012679.
- Onsager, T. G., J. D. Scudder, M. Lockwood, and C. T. Russell (2001), Reconnection at the high-latitude magnetopause during northward interplanetary magnetic field conditions, *J. Geophys. Res.*, *106*, 25,467.
- Paschmann, G., B. Sonnerup, I. Papamastorakis, W. Baumjohann, N. Sckopke, and H. Luehr (1990), The magnetopause and boundary layer for small magnetic shear: Convection electric fields and reconnection, *Geophys. Res. Lett.*, *17*, 1829.
- Paschmann, G., W. Baumjohann, N. Sckopke, T. D. Phan, and H. Luehr (1993), Structure of the dayside magnetopause for low magnetic shear, *J. Geophys. Res.*, *98*, 13,409.
- Phan, T. D., G. Paschmann, A. Raj, V. Angelopoulos, D. Larson, and R. P. Lin (1998), Wind observations of the halo/cold plasma sheet, in *Substorms-4*, edited by S. Kokubun and Y. Kamide, Kluwer Acad., Boston, Mass.
- Phan, T. D., R. P. Lin, S. A. Fuselier, and M. Fujimoto (2000), Wind observations of mixed magnetosheath-plasma sheet ions deep inside the magnetosphere, *J. Geophys. Res.*, *105*, 5497.
- Raeder, J. (1999), Modeling the magnetosphere for northward interplanetary magnetic field: Effects of electrical resistivity, *J. Geophys. Res.*, *104*, 17,357.
- Raeder, J. (2003), Global geospace modeling: Tutorial and review, in *Space Plasma Simulation*, edited by J. Büchner, C. T. Dum, and M. Scholer, Springer, New York.
- Raeder, J., R. J. Walker, and M. Ashour-Abdalla (1995), The structure of the distant geomagnetic tail during long periods of northward IMF, *Geophys. Res. Lett.*, *22*, 349.
- Raeder, J., J. Berchem, M. Ashour-Abdalla, L. A. Frank, W. R. Paterson, K. L. Ackerson, R. P. Lepping, S. Kokubun, T. Yamamoto, and S. A.

- Slavin (1997), Boundary layer formation in the magnetotail: Geotail observations and comparisons with a global MHD model, *Geophys. Res. Lett.*, *24*, 951.
- Raeder, J., J. Berchem, and M. Ashour-Abdalla (1998), The Geospace Environment Modeling grand challenge: Results from a Global Geospace Circulation Model, *J. Geophys. Res.*, *103*, 14,787.
- Raeder, J., R. L. McPherron, L. A. Frank, W. R. Paterson, J. B. Sigwarth, G. Lu, H. J. Singer, S. Kokubun, T. Mukai, and J. A. Slavin (2001), Global simulation of the geospace environment modeling substorm challenge event, *J. Geophys. Res.*, *106*, 381.
- Raeder, J., D. Larson, W. Li, E. L. Kepko, and T. Fuller-Rowell (2008), OpenGGCM simulations for the THEMIS mission, *Space Sci. Rev.*, doi:10.1007/s11,214-008-9421-5.
- Rème, H., et al. (2001), First multispacecraft ion measurements in and near the Earth's magnetosphere with the identical Cluster Ion Spectrometry (CIS) Experiment, *Ann. Geophys.*, *19*, 1303.
- Robinson, R. M., R. R. Vondrak, K. Miller, T. Dabbs, and D. Hardy (1987), On calculating ionospheric conductances from the flux and energy of precipitating electrons, *J. Geophys. Res.*, *92*, 2565.
- Sibeck, D. G., et al. (1999), Plasma transfer processes at the magnetopause, *Space Sci. Rev.*, *88*(1-2), 207.
- Siscoe, G. L., and K. D. Siebert (2003), Local boundary layer properties from non-local processes, in *Earth's Low-Latitude Boundary Layer*, *Geophys. Monogr. Ser.*, vol. 133, edited by P. T. Newell and T. G. Onsager, p. 377, AGU, Washington, D. C.
- Song, P., and C. T. Russell (1992), Model of the formation of the low-latitude boundary layer for strongly northward interplanetary magnetic field, *J. Geophys. Res.*, *97*, 1411.
- Terasawa, T., M. Fujimoto, T. Mukai, I. Shinohara, Y. Saito, T. Yamamoto, S. Machida, S. Kokubun, A. J. Lazarus, and J. T. Steinberg (1997), Solar wind control of density and temperature in the near-earth plasma sheet: WIND/GEOTAIL collaboration, *Geophys. Res. Lett.*, *24*, 935.
- Thomsen, M. F., J. E. Borovsky, R. M. Skoug, and C. W. Smith (2003), Delivery of cold, dense plasma sheet material into the near-Earth region, *J. Geophys. Res.*, *108*(A4), 1151, doi:10.1029/2002JA009544.
- Thorne, R. M., and B. T. Tsurutani (1991), *Physics of Space Plasmas*, *SPI Conference Proceedings and Reprint Series*, vol. 10, Sci. Publ., Cambridge, Mass.
- Treumann, R. A. (1997), Theory of super-diffusion for the magnetopause, *Geophys. Res. Lett.*, *24*, 1727.
- Tsurutani, B. T., G. S. Lakhina, L. Zhang, J. S. Pickett, and Y. Kasahara (2003), ELF/VLF plasma waves in the low latitude boundary layer, in *Earth's Low-Latitude Boundary Layer*, *Geophys. Monogr. Ser.*, vol. 133, edited by P. T. Newell and T. G. Onsager, p. 189, AGU, Washington, D. C.
- Walker, R. J., et al. (1999), Source and loss processes in the magnetotail, *Space Sci. Rev.*, *88*(1-2), 285.
- Walker, R. J., M. Ashour-Abdalla, T. Ogino, V. Perroomian, and R. L. Richard (2003), Modeling magnetospheric sources, in *Earth's Low-Latitude Boundary Layer*, *Geophys. Monogr. Ser.*, p. 133, edited by P. T. Newell and T. G. Onsager, p. 33, AGU, Washington, D. C.
- Wing, S., and P. T. Newell (2002), 2D plasma sheet ion density and temperature profiles for northward and southward IMF, *Geophys. Res. Lett.*, *29*(9), 1307, doi:10.1029/2001GL013950.
- Wing, S., J. R. Johnson, and M. Fujimoto (2006), Timescale for the formation of the cold-dense plasma sheet: A case study, *Geophys. Res. Lett.*, *33*, L23106, doi:10.1029/2006GL027110.
- Yau, A. W., E. G. Shelley, W. K. Peterson, and L. Lenchyshyn (1985), Energetic auroral and polar ion outflow at DE 1 altitudes: Magnitude, composition, magnetic activity dependence, and long-term variations, *J. Geophys. Res.*, *90*, 8417.
- Zhou, X.-Z., Z. Y. Pu, Q.-G. Zong, and L. Xie (2007), Energy filter effect for solar wind particle entry to the plasma sheet via flank regions during southward interplanetary magnetic field, *J. Geophys. Res.*, *112*, A06233, doi:10.1029/2006JA012180.

W. Li and J. Raeder, Space Science Center, University of New Hampshire, Morse Hall, Durham, NH 03824, USA. (wenhuil@cisunix.unh.edu; j.raeder@unh.edu)

M. Øieroset and T. D. Phan, Space Sciences Laboratory, University of California, Berkeley, CA 94720, USA. (oieroset@ssl.berkeley.edu; phan@ssl.berkeley.edu)